Available online at www.sciencedirect.com
SCIENCE DIRECT®
International Journal of Thermal Sciences 43 (2004) 817–823
International Journal of Thermal Sciences
www.elsevier.com/locate/ijts

Temporal evolution of thermal convection in an initially stably-stratified horizontal fluid layer

Chang Kyun Choi [a,*], Joung Hwan Park [a], Hee Kwan Park [a], Hong Je Cho [a], Tae Joon Chung [a], Min Chan Kim [b]

[a] *School of Chemical Engineering, Seoul National University, Seoul 151-744, South Korea*
[b] *Department of Chemical Engineering, Cheju National University, Cheju 690-756, South Korea*

Received 20 August 2003; received in revised form 18 January 2004; accepted 24 February 2004

Available online 25 May 2004

Abstract

The temporal evolution of buoyancy-driven convection in an initially quiescent and stably-stratified fluid layer confined between two horizontal plates is investigated theoretically. After the temperature of the bottom plate is increased suddenly to a higher one, buoyancy-driven convection appears at a certain time. In order to trace the related time-dependent thermal behavior, the Boussinesq equations are solved numerically by using the finite element method to examine the growth rates of the basic temperature field and its fluctuations with time. Based on the numerical results, the characteristic times to mark the onset of intrinsic instability, the first detection of convective motion and the ensuing manifestation of convection are illustrated by a set of new parameters suggested here. The latter two characteristic times are discussed in comparison with the experimental data available in the literature.

Keywords: Buoyancy-driven convection; Detection time of motion; Fluctuations; Intrinsic instability; Propagation theory; Temporal growth rate; Undershoot time

1. Introduction

Natural convection is encountered in a variety of industrial systems involving heat and mass transfer, as well as in nature. The related convective instabilities have been investigated extensively since the beginning of the 20th century [1, 2]. But, in a rapidly developing and nonlinear temperature field the related instability phenomenon still remains unresolved because of its inherent complexity.

In horizontal fluid layers heated rapidly from below buoyancy-driven convection appears at a certain time. In such transient systems it is important to predict the characteristic time, t_c, to mark the onset of convective instability, i.e., intrinsic instability. For times $t \geqslant t_c$, dangerous instabilities can grow until the first convective motion is detected at $t = t_D$. Then, an undershoot time, t_u, in the plot of the heating rate versus time will be observed, which indicates the deviation of the Nusselt number from that in the conduction state. Morton [3], Foster [4], Jhaveri and Homsy [5], Tan and Thorpe [6], and Choi et al. [7,8] conducted the related instability analysis by using, respectively, the frozen-time model, amplification theory, stochastic model, maximum-Rayleigh number criterion, and propagation theory.

In the present study, the onset of convective motion in an initially quiescent and stably stratified fluid layer between two horizontal plates is analyzed. This specific problem was analyzed based on the amplification theory by Ueda et al. [9], who measured the detection time t_D by flow visualization and also temperature measurement. Kim et al. [10] analyzed the same problem based on the propagation theory, which deals with the instability problems of developing and nonlinear temperature profiles for large Rayleigh numbers. It has been shown that for large-Prandtl systems the experimental undershoot time is approximately four times larger than the predicted critical time for the onset of the fastest growing instability. But, the above analyses based on the amplification and the propagation theories require a further justification. Accordingly, in the present study we have employed the finite element method (FEM) to identify the char-

* Corresponding author. Fax: 82-2-888-7295.
E-mail address: ckchoi@snu.ac.kr (C.K. Choi).

1290-0729/$ – see front matter
doi:10.1016/j.ijthermalsci.2004.02.022

Nomenclature

a	dimensionless horizontal wavenumber
A, B	amplitudes of temperature and velocity fluctuations
E_0	energy identity of mean fields
E_1	energy identity of fluctuations
H	thickness of the fluid layer ..... m
Nu	Nusselt number
p	dimensionless pressure, $= PH^2/(\rho\alpha^2)$
P	dynamic pressure ..... $\mathrm{N\cdot m^{-2}}$
Pr	Prandtl number, $= \nu/\alpha$
Ra	modified Rayleigh number, $= g\beta(T_b - T_i)H^3/(\alpha\nu)$
r_0	temporal growth rate of mean fields
r_1	temporal growth rate of fluctuations
S	area of the bottom plate ..... $\mathrm{m^2}$
t	time ..... s
T	temperature ..... K
T_b	temperature of the bottom plate ..... K
T_i	initial temperature of the bottom plate ..... K
T_u	temperature of the upper plate ..... K
ΔT	step change in the bottom temperature, $= T_b - T_i$ ..... K
$\mathbf{u}$	dimensionless velocity vector, $= u\hat{\mathbf{i}} + v\hat{\mathbf{j}} + w\hat{\mathbf{k}}$
$\mathbf{U}$	velocity vector ..... $\mathrm{m\cdot s^{-2}}$
w	dimensionless vertical velocity
x, y, z	dimensionless Cartesian coordinates
Z	vertical distance ..... m

Greek symbols

α	thermal diffusivity ..... $\mathrm{m^2\cdot s^{-1}}$
β	thermal expansion coefficient ..... $\mathrm{K^{-1}}$
Δ_T	thermal penetration depth ..... m
γ	temperature ratio, $= (T_u - T_i)/(T_b - T_i)$
ν	kinematic viscosity ..... $\mathrm{m^2\cdot s^{-1}}$
θ	dimensionless temperature, $= (T - T_i)/\Delta T$
ρ	fluid density ..... $\mathrm{kg\cdot m^{-3}}$
τ	dimensionless time, $= \alpha t/H^2$
τ_D	dimensionless detection time of motion
τ_m	dimensionless time when r_1 reaches the maximum
τ_u	dimensionless undershoot time

Subscripts

c	critical state
D	detection
rms	root-mean-square quantity
0	basic state of conduction
1	perturbed state
$*$	normalized fluctuation

Superscripts

$*$	amplitude function or propagation theory
$'$	fluctuation

acteristic times (t_c, t_D, t_u) to a certain degree in comparison with the experimental results of Ueda et al. [9].

2. Onset of convective instability

The system considered here is an initially stably-stratified horizontal fluid layer of thickness H, as shown in Fig. 1. For times $t \leqslant 0$, the conduction field has a linear temperature profile with $T = T_i$ at $Z = 0$ and $T = T_u$ at $Z = H$. The fluid layer is heated from below to a higher temperature T_b ($> T_i$) at $Z = 0$ for $t > 0$. The important parameters describing the present system are the Prandtl number Pr, the modified Rayleigh number Ra, and the temperature ratio γ. For a high ΔT ($= T_b - T_i$), the nonlinear developing temperature

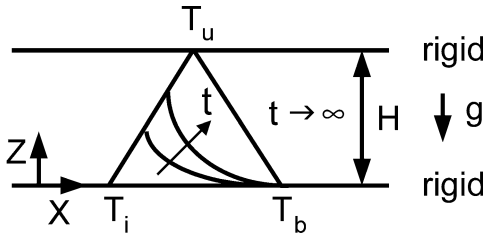

Fig. 1. Temperature profiles in conduction state.

profiles of the conduction regime are formed and then a buoyancy-driven convection sets in at a certain time. The governing equations of the flow and temperature fields in the convection regime can be expressed in dimensionless form with the Boussinessq approximation as follows:

$$\nabla \cdot \mathbf{u} = 0 \tag{1}$$

$$\left(\frac{\partial}{\partial \tau} + \mathbf{u}\cdot\nabla\right)\mathbf{u} = -\nabla p + Pr\,\nabla^2\mathbf{u} + Pr\,Ra\,\theta\hat{\mathbf{k}} \tag{2}$$

$$\left(\frac{\partial}{\partial \tau} + \mathbf{u}\cdot\nabla\right)\theta = \nabla^2\theta \tag{3}$$

with the boundary conditions,

$$\mathbf{u} = \frac{\partial \mathbf{u}}{\partial z} = \mathbf{0}, \quad \theta = 1 \quad \text{at } z = 0 \tag{4a, b}$$

$$\mathbf{u} = \frac{\partial \mathbf{u}}{\partial z} = \mathbf{0}, \quad \theta = \gamma \quad \text{at } z = 1 \tag{5a, b}$$

where θ, p, τ, and $\mathbf{u}$ denote, respectively, the dimensionless forms of the temperature T, the dynamic pressure P, and the velocity vector $\mathbf{U}$. Here, $\hat{\mathbf{k}}$ represents the vertical unit vector, the fluid density ρ used is the value at $T = T_i$, and the dimensionless Cartesian coordinates (x, y, z) have the scale of H.

As it is well known, at the fully-developed state thermal convection exists for $Ra(1 - \gamma) \geqslant 1708$ with $\gamma < 1$. For

$\gamma = 1$, the fully-developed state becomes an isothermal one. For $\gamma > 1$, the upper boundary temperature is higher than the lower one and, therefore, incipient motion will disappear as $\tau \to \infty$. But, for a large *Ra* the transient motion sets in at a certain time.

For a low *Ra*, the incipient convective instabilities are well illustrated by the propagation theory, which model employs the normal-mode analysis under linear theory. Infinitesimal disturbances are assumed to exhibit the horizontal periodicity, and the dimensionless vertical velocity disturbance w_1 and the dimensionless temperature disturbance θ_1 can be expressed as

$$\begin{aligned}&\big[w_1(\tau,x,y,z),\theta_1(\tau,x,y,z)\big]\\&\quad=\big[w_1^*(\tau,z),\theta_1^*(\tau,z)\big]\exp\big[i(a_x x+a_y y)\big]\end{aligned}\tag{6}$$

where i is the imaginary unit and the dimensionless horizontal wavenumber a has the relation of $a=[a_x^2+a_y^2]^{1/2}$. The propagation theory is based on the assumption that in deep-pool systems the incipient temperature disturbances are propagated mainly within the thermal penetration depth Δ_T at the onset time of thermal instability. Therefore, all the variables and parameters having the length scale are rescaled with Δ_T. The self-similar transformations are forced and, therefore, the stability criteria are obtained easily. For the present system, the resulting τ_c- and a_c-values have been illustrated by Kim et al. [10]. In the present study, their τ_c-values are referred to τ_c^*. Since this model does not provide τ_D, or τ_u, explicitly, we have employed the numerical method here.

3. Numerical simulation

3.1. FEM

We have solved the governing equations (1)–(3) by using the Galerkin finite element method, and only considered a two-dimensional cellular motion with horizontal periodicity. Accordingly, one convection cell was chosen, the side boundaries of which were assumed to have stress free and adiabatic conditions describing the horizontally infinite layer. The penalty function method was applied to solve the pressure velocity coupling, where the pressure and the continuity equation are related by the relation $p=-\lambda(\partial v/\partial y+\partial w/\partial z)$. To satisfy the convergence condition, the penalty number λ was fixed to $Pr\times10^8$. In order to solve this transient problem, the implicit predictor/multicorrector algorithm associated with the Newton–Raphson scheme was adopted and the first-order time increment was used. The number of elements was 40×36 and finer meshes were used near the top and bottom boundaries to guarantee the physical validity. Also, to ensure the numerical stability, a time step of $\Delta\tau=10^{-5}$ was used. In the associated Newton–Raphson scheme, the convergence was assumed when the norm of residuals and correctors was smaller than 10^{-5} at each time step.

3.2. Averaged equations and fluctuations

The velocity and temperature fields can be described by

$$\mathbf{u}=\langle\mathbf{u}\rangle+\mathbf{u}'\tag{7}$$

$$\theta=\langle\theta\rangle+\theta'\tag{8}$$

where $\langle\cdot\rangle$ denotes the horizontal means, with $\mathbf{u}'$ and θ' being the velocity and temperature fluctuations, respectively. With their extremely small values, they lead to w_1 and θ_1 in Eq. (6), and it is known that $\langle\mathbf{u}\rangle=0$.

For the present time-dependent problem the selection of the initial conditions is very important. The two-dimensional fluctuations are assumed to show periodic patterns like Eq. (6):

$$\begin{aligned}&\big[\theta',\mathbf{u}'\big]\cong\big[A(\tau)\theta_*(z),B(\tau)\mathbf{u}_*(z)\big]\exp\big[i(ay)\big]\\&\quad\text{for } 0\leqslant\tau\leqslant\tau_c\end{aligned}\tag{9}$$

where A and B are the amplitudes. Here θ_* and $\mathbf{u}_*$ represent the normalized temperature and velocity fluctuations, respectively. The initial conditions constructed at $\tau=0$ are: $\theta'=A(0)\theta_*(z)\cos(ay)$, $v'=B(0)(\partial w_*(z)/\partial z)a\sin(ay)$ and $w'=B(0)w_*(z)\cos(ay)$, where $A(0)$ and $B(0)$ are the initial amplitudes of the fluctuations. The calculations were initiated with the stability criteria obtained from the propagation theory [10]. But, it was assumed that $\theta_*(z)$ and $w_*(z)$ would not change during $0\leqslant\tau\leqslant\tau_c$, which means that the unique disturbance patterns are decided with the converged τ_c-value during $0\leqslant\tau\leqslant\tau_c$ by iterating the calculations with the newly obtained patterns. Since we do not know the actual initial conditions, the numerical quantities for $\tau<\tau_c$ may not represent the actual phenomena, but the critical ones at $\tau=\tau_c$ should be valid.

3.3. Onset of intrinsic instability

Based on the above notations of velocity and temperature fields, the energy identities can be expressed as

$$E_0=\frac{1}{2}\int_V\big(\langle u\rangle^2+\langle v\rangle^2+\langle w\rangle^2+b\,Pr\,Ra\langle\theta\rangle^2\big)\,\mathrm{d}V\tag{10}$$

$$E_1=\frac{1}{2}\int_V\big(u'^2+v'^2+w'^2+b\,Pr\,Ra\,\theta'^2\big)\,\mathrm{d}V\tag{11}$$

where E_0 is the energy identity of the mean fields, and E_1 is that of its fluctuations, which are function of time only. Furthermore, V represents the volume of the system considered. In the energy method, which has been well illustrated by Joseph [11], $b=1$ is usually adopted. In order to observe the time-dependent behavior of thermal convection, the following temporal growth rates of the above energy identities are defined:

$$r_0=\frac{1}{E_0^{1/2}}\frac{\mathrm{d}E_0^{1/2}}{\mathrm{d}\tau}\tag{12}$$

$$r_1 = \frac{1}{E_1^{1/2}} \frac{\mathrm{d}E_1^{1/2}}{\mathrm{d}\tau} \tag{13}$$

For $Pr \to \infty$, the kinetic energy in Eqs. (10) and (11) is relatively very small and, therefore, the temporal growth rates of the energy identities reduce to

$$r_0 = \frac{1}{\langle\theta\rangle_{\mathrm{rms}}} \frac{\mathrm{d}\langle\theta\rangle_{\mathrm{rms}}}{\mathrm{d}\tau} \tag{14}$$

$$r_1 = \frac{1}{\theta'_{\mathrm{rms}}} \frac{\mathrm{d}\theta'_{\mathrm{rms}}}{\mathrm{d}\tau} \tag{15}$$

where the subscript 'rms' refers to the root-mean-square quantity. These quantities may be called the growth rates of the averaged temperature and that of temperature fluctuations. Similarly, we define w'_{rms} as the root-mean-square quantity of w'. The amplification factor in the amplification theory is usually defined as the ratio of w'_{rms} to its initial value.

Here, we suggest that the critical condition of the onset of intrinsic instability is represented by

$$r_1 = r_0 \quad \text{at } \tau = \tau_c \tag{16}$$

which means that the characteristic cellular motion of $a = a_c$ that would satisfy equations (9) and (16) would set in at the converged earliest time τ_c. It should, however, be noted that the stability criteria from the propagation theory satisfy the condition of $r_1 = r_0$ at $\tau = \tau_c^*$. With $\gamma = 0$, r_0 approaches $1/(4\tau)$ for $\tau \to 0$. The system is assumed stable with $r_1 < r_0$ but unstable $r_1 > r_0$. In the frozen-time model, the system is stable with $r_1 < 0$ and the thermal instability sets in with $r_1 = 0$.

3.4. Undershoot time

In the present study, the Nusselt number is defined as follows:

$$Nu = \frac{1}{S} \int_S \left(-\frac{\partial\theta}{\partial z} \right)_{z=0} \mathrm{d}S \tag{17}$$

where S is the surface area of the bottom plate and the characteristic length is the layer depth H. When heat transfer is controlled by conduction only, Nu approaches $(1 - \gamma)$ as $\tau \to \infty$. But with strong convection, Nu deviates from its conduction solution and has a minimum at $\tau = \tau_u$ The undershoot time, τ_u, is frequently used as the characteristic time to represent detection of convection regime.

3.5. Simulation

With the initial temperature amplitude of $A(0) = 10^{-3}$, the present system was simulated numerically for a given Ra and γ with $Pr \to \infty$. The above $A(0)$-value yields the maximum w- and the Nu-values, which agree well with the available experimental data for the fully developed state for $Ra < 10^4$ with $\gamma = 0$. Also, the linearized governing equations were solved and the results were compared with the nonlinear ones. The related equations are described in detail in the work of Kim et al. [10].

4. Results and discussion

The numerical simulation results by the FEM with $Pr \to \infty$ and $A(0) = 10^{-3}$ are reported here. Based on Eqs. (14) and (15), the stability criteria to satisfy the condition (16) are assumed to represent the fastest growing, two-dimensional instability in the form of regular cells.

For $Ra = 10^5$, the growth behavior of fluctuations is shown in Fig. 2. For small τ, w'_{rms} and θ'_{rms} have each almost the same magnitudes as their initial ones. But starting from a certain time, they experience a sudden increase to a maximum before they decrease with time. With $\gamma = 0.6$, the growing process is delayed but the earlier behavior of θ'_{rms} is almost the same as that of $\gamma = 0$. Mahler and Schechter [12] mentioned that a reasonable choice of initial conditions would be a representation in which there is no tendency for the initial velocity perturbation to either grow or decay. The present results are supported to a certain degree by their statement.

The typical temporal behavior given by Eqs. (14)–(17) are illustrated in Figs. 3 and 4. The condition (16) yields $\tau_c = 3.18 \times 10^{-3}$ and $a_c = 10.1$ for $Ra = 10^5$ and $\gamma = 0.6$, as shown in Fig. 3. The r_1-value reaches the maximum at $\tau = \tau_m$. Up to this characteristic time the results obtained from the linear theory are almost the same as the present ones. Even after $\tau = \tau_m$, the former r_1-value continues to increase with time. The corresponding τ_u-values are seen in Fig. 4. The above figures show that the characteristic times increase with decreasing Ra. Since $\tau_m \leqslant \tau_u$ ensuing convection is observed at $\tau = \tau_u$.

A peculiar behavior, however, is shown in Fig. 5. With $Ra = 15000$ and $\gamma = 0.9$, the growing thermal instability

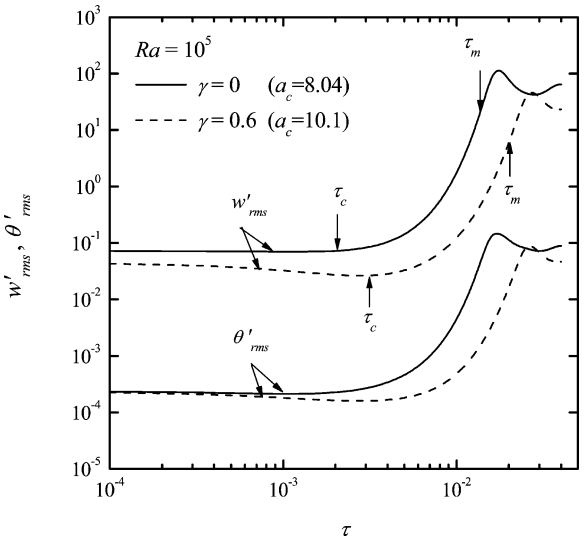

Fig. 2. Temporal behavior of temperature and velocity fluctuations. At $\tau = \tau_m$, the r_1-value is the maximum.

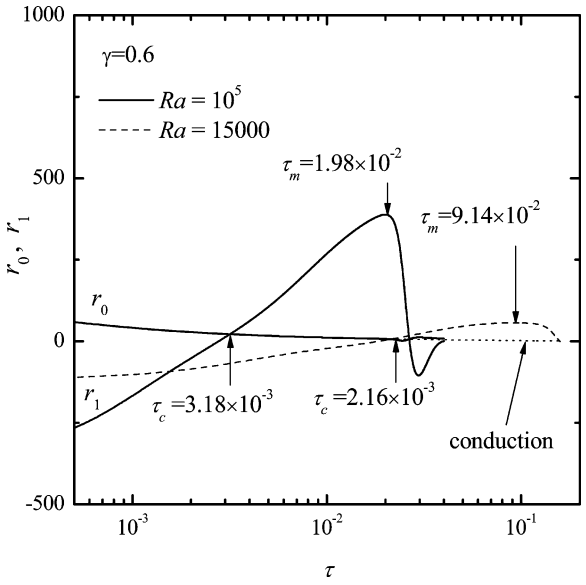

Fig. 3. Temporal growth rates with time: τ_c, onset time of intrinsic instability; τ_D, detection time of convective motion ($\cong \tau_m$).

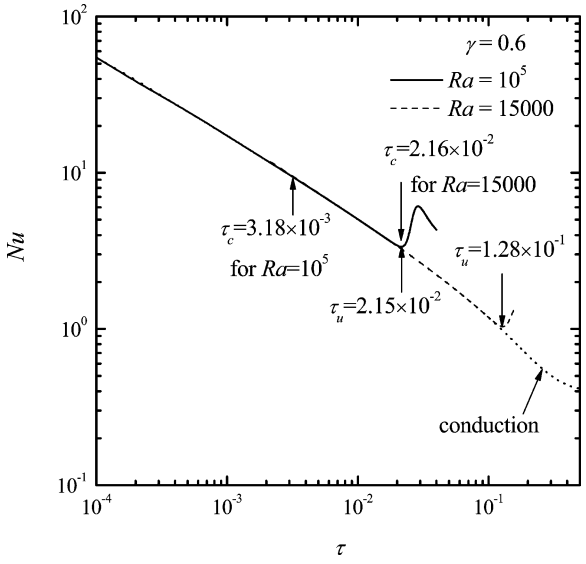

Fig. 4. Nusselt number versus time: τ_c, onset time of intrinsic instability; τ_u, undershoot time.

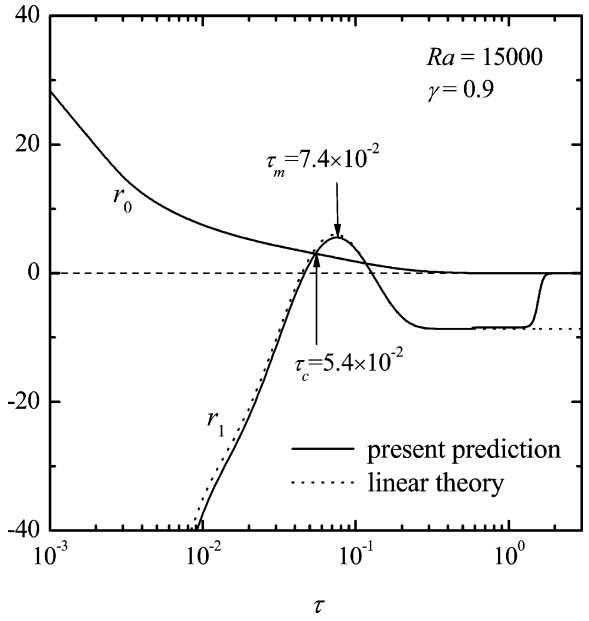

Fig. 5. Peculiar behavior of temporal growth rates for $\gamma = 0.9$, wherein $Ra(1-\gamma) < 1708$.

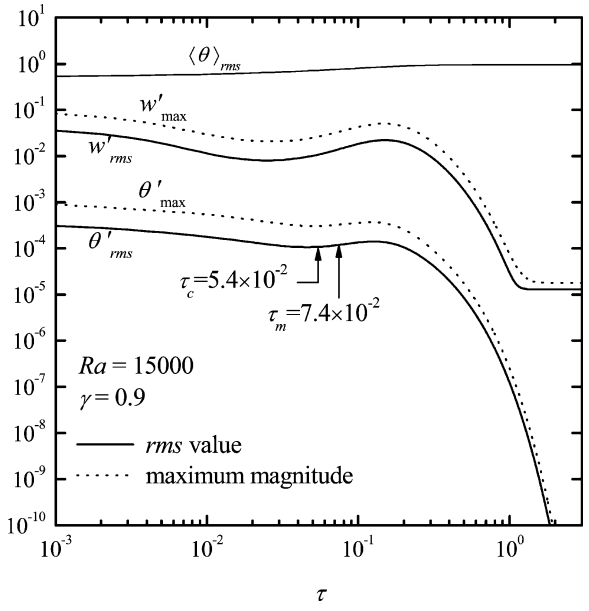

Fig. 6. Peculiar behavior of fluctuations for $\gamma = 0.9$. The r_1-value is the maximum at $\tau = \tau_m$.

sets in at $\tau = 5.4 \times 10^{-2}$. It first grows and then decays with time. Finally, convective motion disappears as $\tau \to \infty$. It is noted that with $\gamma = 0.9$, as $\tau \to \infty$, $Ra(1-\gamma) = 1500$, which is smaller than the well-known critical Rayleigh number 1708, and $Nu = 1 - \gamma$. The value 1708 is obtained by using the temperature difference $T_b - T_u$ instead of ΔT in the modified Rayleigh number. Up to $\tau = 1.0$, the linear theory yields almost the same r_1-value as that from the nonlinear equations, as shown in Fig. 5. In this case, τ_u is not clear in the plot of Nu vs. τ, where τ_u becomes meaningless. The temporal behaviors of w'_{rms} and θ'_{rms} are shown in Fig. 6, with which the maximum magnitudes of w' and θ', i.e., w'_{max} and θ'_{max}, are compared. It is known that their trends are almost the same. Even though the maximum magnitude of fluctuations at $\tau = 10^{-3}$ is a little larger than that at $\tau = \tau_c$, the domain of $r_1 < r_0$ is here said to be stable. The strange behaviors of w'_{rms} and θ'_{rms} at the earlier stage are also seen for $Ra = 10^5$ and $\gamma = 0.6$ in Fig. 2. It is known that the present simulation becomes valid as $\tau \to \tau_c$. For $Pr \to \infty$, the effect of the initial velocity magnitude $B(0)$ in Eq. (9) on τ_c and θ'_{rms} is not significant.

With increasing γ, the τ_m/τ_c-value decreases but the τ_u/τ_c-ratio increases. Comparing the τ_m-value in Fig. 3 with that in Fig. 5, we suggest that $\tau_D \cong \tau_m$ because the result from the linear theory deviates from the nonlinear one

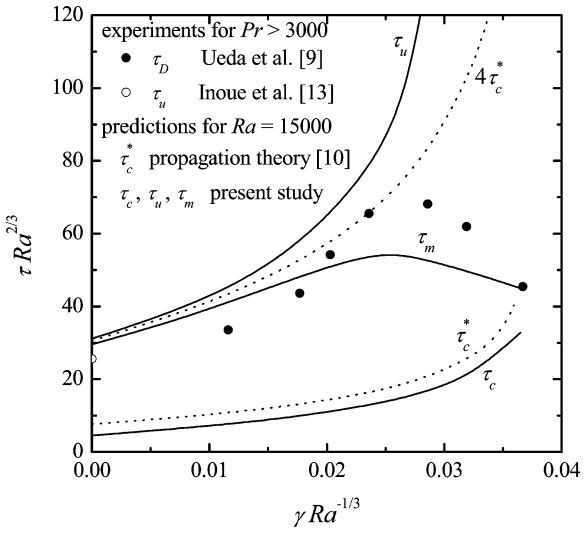

Fig. 7. Comparison of predictions with available experimental data, wherein $\tau_c < \tau_m \leqslant \tau_u$: τ_c onset time of intrinsic instability; τ_u, undershoot time. At $\tau = \tau_m$, the r_1-value is the maximum.

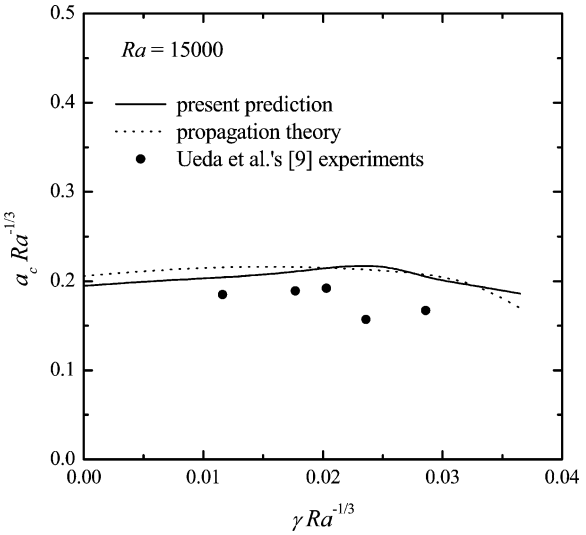

Fig. 8. Comparison of critical wavenumbers between numerical and experimental data.

near $\tau = \tau_m$ in the former case. This means that convective motion can be detected earlier at $\tau = \tau_D$ ($\leqslant \tau_u$).

Ueda et al. [9] measured τ_D-values by using aluminum powders for $\gamma = 0.73$–1.67, $Pr = 8800$ and $Ra = 9000$–$17\,000$, as shown in Fig. 7. Their predictions from the amplification theory agree reasonably well with their experimental data, but their amplification factor is not a decisive one. The experimental data of Inoue et al. [13] for $\gamma = 0$ are also shown in Fig. 7. The above experimental environments may be considered as those of $Pr \to \infty$. The predictions of Kim et al. [10] represented by τ_c^* is located near τ_c. This means that for $Ra \leqslant 15\,000$ the stability criteria from the propagation theory are almost the same as the present ones. But, it is noted that with increasing Ra the difference between these two predictions becomes relatively larger. Foster [14] suggested the relation of $\tau_D \cong 4\tau_c$, which agrees reasonably well with τ_u and τ_m for $\gamma Ra^{-1/3} \leqslant 0.02$. With increasing γ for $0.6 < \gamma < 1$, the τ_D- and τ_m-values decrease and the difference between τ_c and τ_u becomes larger. In this γ-range, it may be stated that, for a given Ra, convective motion is detected earlier with increasing γ. This peculiar behavior supports the relation of $\tau_D \cong \tau_m$. The present a_c-value is compared with the experimental value of Ueda et al. [9] and that from the propagation theory in Fig. 8. The agreement is good because the γ-effect on the cell size is not significant for $Ra \cong 15\,000$.

The present τ_c-value does not vary for a given set of Ra, Pr and γ values but the τ_m- and τ_u-values decrease with increasing the $A(0)$-value for $\gamma = 0$. The present simulation with $A(0) = 10^{-3}$ seems to reasonably represent actual processes of large Pr for $\tau \geqslant \tau_c$ (see the case of $\gamma = 0$ in Fig. 7). But we do not know what kind of initial conditions exist at $\tau = 0$. It is believed that thermal instabilities are triggered by thermal noises. These microscopic noises will appear as fluctuations of the macroscopic velocity and temperature fields. Therefore, the present simulation results are not valid before definitive fluctuations appear. When fluctuations grow while the basic field is growing more rapidly, then fluctuations would appear to be decaying. This concept supports the instability criterion (16). From the above considerations it is stated that the results from the present model are valid for $\tau_c \leqslant \tau \leqslant \tau_m$. For extremely small-$Pr$ systems, r_1 would not be represented by Eq. (15) since the effect of the kinetic energy on τ_c becomes dominant. Therefore, this equation should be used for large-Pr systems. It is stressed that at $\tau = \tau_c$ the convective instability driven by thermal noises is rarely detectable by eye and should grow until convective motion is detected at $\tau = \tau_D$. The convective motion is related to the velocity fields. Therefore, it seems that τ_D is decided by the kinetic energy identity ($b = 0$ in Eq. (11)). For $Pr \to \infty$, the r_1-behavior with $b = 0$ is almost the same as the thermal one. For small Pr, the kinetic effect would be decisive in detection of convective motion. The decision of the b-value for a finite Pr requires a further justification.

5. Conclusion

For $Pr \to \infty$, the critical time to mark the onset of convective instability in the conduction regime shown in Fig. 1 has been investigated by using the FEM with $A(0) = 10^{-3}$. This $A(0)$-value produces the τ_u-value in agreement with the experimental one for $Ra \geqslant 10^5$ with $\gamma = 0$. It is suggested that in the present system a fastest growing mode of regular cells would set in at $\tau = \tau_c$ with $r_0 = r_1$. Here τ_c has been called the onset time of intrinsic instability because it is invariant, which is independent of the $A(0)$-value, for a given set of values of Ra, Pr and γ. Since the linear theory is applied up to $\tau \cong \tau_m$ ($\leqslant \tau_u$), manifest convection is surely observed at $\tau = \tau_u$. But convective motion can

be detected earlier at $\tau = \tau_D$ ($\leqslant \tau_u$) and, therefore, we suggest that $\tau_D \cong \tau_m$. For $Ra = 15\,000$ and $Pr \to \infty$, the τ_m-value has the maximum near $\gamma = 0.6$ which is consistent with the available experimental data. For $0.6 < \gamma < 1$, it is known that the τ_m/τ_c-value decreases with increasing γ. The present numerical simulation follows the actual phenomena reasonably well for $\tau_c \leqslant \tau \leqslant \tau_u$ and clarifies the meaning of τ_c, τ_D and τ_u to a certain degree.

Acknowledgements

This work was supported by LG Chemical Ltd., Seoul under the Brain Korea 21 Project of the Ministry of Education.

References

[1] H. Bénard, Les tourbillons cellulaires dans une nappe liquide transportant de la chaleur par convection en régime permanent, Ann. Chem. Phys. 23 (1901) 62–144.
[2] Lord Rayleigh, On convection currents in a horizontal layer of fluid when the higher temperature is on the under side, Philos. Mag. 32 (1916) 529–546.
[3] B.R. Morton, On the equilibrium of a stratified layer of fluid, J. Mech. Appl. Math. 10 (1957) 433–447.
[4] T.D. Foster, Stability of homogeneous fluid cooled uniformly from above, Phys. Fluids 8 (1965) 1249–1257.
[5] B.S. Jhaveri, G.M. Homsy, The onset of convection in fluid layer heated rapidly in a time-dependent manner, J. Fluid Mech. 114 (1982) 251–260.
[6] K.K. Tan, R.B. Thorpe, The onset of convection caused by buoyancy during transient heat conduction in deep fluids, Chem. Engrg. Sci. 51 (1996) 4127–4136.
[7] C.K. Choi, K.H. Kang, M.C. Kim, Convective instabilities and transport properties in horizontal fluid layers, Korean J. Chem. Engrg. 15 (1998) 192–198.
[8] D.J. Yang, C.K. Choi, The onset of thermal convection in a horizontal fluid layer heated from below with time-dependent heat flux, Phys. Fluids 14 (2002) 930–937.
[9] H. Ueda, S. Komori, T. Miyazaki, H. Ozoe, Time-dependent thermal convection in a stably stratified fluid layer heated from below, Phys. Fluids 27 (1984) 2617–2623.
[10] M.C. Kim, H.K. Park, C.K. Choi, Stability of an initially, stably stratified fluid subjected to a step change in temperature, Theor. Comp. Fluid Dyn. 16 (2002) 49–57.
[11] D.D. Joseph, Stability of Fluid Motions, I and II, Springer, New York, 1976.
[12] E.G. Mahler, R.S. Schechter, The stability of a fluid layer with gas absorption, Chem. Engrg. Sci. 25 (1970) 955–968.
[13] Y. Inoue, S. Akutagawa, S. Saeki, R. Ito, Bénard convection of electrolytic solution in electric field, Kagaku Kogaku Ronbunshu 9 (1983) 359–369.
[14] T.D. Foster, Onset of manifest convection in a layer of fluid with time-dependent surface temperature, Phys. Fluids 12 (1969) 2482–2487.